Evaluation of Viscoplastic Parameters of an Austenitic Stainless Steel at High Temperature

A.K. Asraff, Merin V. George, Krishnajith Jayamani and S. Sarath Chandran Nair

Abstract Metals at high temperatures are sensitive to strain rate effects and exhibit viscoplastic behavior. The Perzyna model is one of the most widely used ones to study rate-dependent plasticity. This paper presents the details of calibration of Perzyna model parameters of an austenitic stainless steel from tension tests and calibration of Chaboche and Voce model parameters from low-cycle fatigue test at 1000 K. Tests are conducted in an INSTRON 8862 electromechanical UTM. Perzyna model parameters are validated by comparing tension test results with finite element simulations using ANSYS (Version 16.0) software. Sensitivity of Perzyna model parameters on viscoplastic behavior is investigated for monotonic as well as cyclic loading situations. Perzyna model is combined with the Chaboche–Voce cyclic plasticity model for investigating cyclic loading. Finally, viscoplastic cyclic stress analysis of a double-walled rocket engine thrust chamber is carried out using a combination of Perzyna, Chaboche and Voce models and its cyclic life evaluated.

Keywords ANSYS · Chaboche model · Voce model · Perzyna model
Stainless steel · UTM · Viscoplasticity

1 Introduction

Plasticity in metals can be classified into two: classical plasticity which is time independent and viscoplasticity which is time or rate dependent. For time-dependent plasticity, the stress–strain behavior is dependent on rate of loading and whether the loading is strain- or stress-controlled [1]. Viscoplasticity in metals

A.K. Asraff (✉) · K. Jayamani · S. Sarath Chandran Nair
Structural Dynamics & Analysis Group, Liquid Propulsion Systems Centre, ISRO, Trivandrum, India
e-mail: akasraff@yahoo.com

M.V. George
Department of Civil Engineering, Mar Athanasius College of Engineering, Kothamangalam, Ernakulam, India

S. Seetharamu et al. (eds.), *Proceedings of Fatigue, Durability and Fracture Mechanics*, Lecture Notes in Mechanical Engineering, https://doi.org/10.1007/978-981-10-6002-1_2

is observed when the operating temperature is above 0.5 T_m where T_m is the melting point in kelvin. The strain rate effect is also significant under dynamic loading [2]. Most theories of viscoplasticity are formulated by adding the strain rate effects to classical theory of plasticity. The total strain rate may be additively decomposed into elastic and inelastic parts as given in Eq. 1:

$$\dot{\varepsilon} = \dot{\varepsilon}^e + \dot{\varepsilon}^i \tag{1}$$

where $\dot{\varepsilon}^e$ represents the elastic effects and $\dot{\varepsilon}^i$ represents combined viscous and plastic effects. It is important to note that in this equation, viscous and plastic effects cannot be separated and are combined together.

The behavior of structures operating at elevated temperatures beyond the yield limit requires taking into account material viscosity and hardening properties. For modeling the rate-dependent plastic deformation of metals and alloys, two types of constitutive equations have been used. In one approach, no yield surface is assumed and plastic deformation starts from the onset of loading although its value might be negligible under certain levels of stress. This approach is usually referred to as the unified creep plasticity theory because there is no separation between time-dependent (creep) and time-independent deformations. In the second approach, a yield surface is assumed after which plastic deformation develops. Viscoplastic models fall in this category. This approach uses the notion of static yield surface and dynamic loading surface. The positive difference between the current dynamic stress and corresponding static stress is known as the overstress measure [3]. The fundamental empirical equation of Cowper and Symonds provides the simplest description of dynamic behavior of a viscoplastic material (see Eq. 2).

$$\frac{\sigma_d}{\sigma_s} = 1 + \left(\frac{\dot{\varepsilon}}{D}\right)^m \tag{2}$$

where σ_d is the rate-dependent or dynamic yield stress, σ_s is the static yield stress (yield stress at zero strain rate), $\dot{\varepsilon}$ is the strain rate, D has the same unit as that of strain rate and is called the material viscosity parameter. m is called the material strain rate hardening parameter and $0 < m < 1$. The ratio of dynamic yield stress to static yield stress (σ_d/σ_s) is known as 'stress ratio' [4]. In order to describe viscoplastic behavior, many constitutive laws have been developed, Anand [5], Perzyna [6] and Chaboche [7, 8] being some of them. Out of these, Perzyna model is one of the simplest ones. Yang and Luo [9] conducted a series of tensile experiments at a single temperature and different strain rates as well as under the same strain rate and different temperatures on carbon constructional quality steels, and the experimental results were analyzed theoretically. Furthermore, the rheological models of carbon steels were built combining the strong points of Perzyna and Johnson–Cook models. Results proved that the model can reflect the temperature effect and strain rate effect of these steels better. Safari et al. [2] developed a constitutive equation for austenitic stainless steel 310S at high temperature taking into account viscosity and strain rate effects. For this, the authors performed both

static and dynamic tension tests at various temperatures. To verify the model, the tension test results were compared with numerical results using ABAQUS program. Kłosowski and Mleczek [10] dealt with identification of parameters for Perzyna and Chaboche viscoplastic models for aluminum alloy at elevated temperature. Results of these were verified by numerical simulation of the laboratory tests. The material parameters were calculated on the basis of uniaxial tension test. The authors emphasized that a simple constitutive law like Perzyna model can very well represent viscoplastic material behavior. Yang et al. [11] conducted detailed viscoplastic structural analysis of a double-walled thrust chamber wall to study its damage process, phase by phase. Analysis revealed that under the same level of thermal structural loading, the duration of startup and shutdown phases plays an important role in the stress and strain evolution.

In this work, a series of tension tests are conducted on specimens made of austenitic stainless steel at 1000 K and different strain rates. From the test results, the viscoplastic parameters are determined by curve fitting based on the procedure developed by Kłosowski and Mleczek [10]. Sensitivity of different model parameters is investigated for monotonic and cyclic loadings from finite element simulations. Cyclic plasticity model parameters of the material are calibrated from LCF tests. The Chaboche–Voce model combination has been used for cyclic plastic modeling. Two-dimensional finite element modeling and cyclic stress analysis of a double-walled thrust chamber has been conducted using a combination of Perzyna, Chaboche and Voce models and its cyclic life evaluated.

2 Viscoplastic Models in ANSYS

The following viscoplastic models are available in ANSYS [5]: (1) Anand model, (2) Pierce model, (3) Perzyna model and (4) Chaboche model. This work uses the Perzyna viscoplastic model. It has to be combined with a suitable classical plasticity model to represent the elastoplastic part. The Perzyna model is obtained by rearranging the basic Cowper and Symonds equation as follows:

$$\dot{\varepsilon} = D\left(\frac{\sigma_d}{\sigma_s} - 1\right)^{1/m} \tag{3}$$

The parameters D, m and σ_s are evaluated by curve fitting from tension tests at the desired temperature [10].

3 Tensile Testing of Austenitic Stainless Steel

Tensile tests are conducted in an INSTRON 8862 electromechanical UTM. Photograph of the machine is shown in Fig. 1. Salient features of the machine are listed below:

- Load frame rating: 100 kN
- Test temperature range: 30–1400 °C
- Induction heating system
- Water-cooled environment chamber inside which tests can be conducted
- Argon purging system
- Water-cooled pull rods.

Tests are done at 1000 K (727 °C) and strain rates of 1×10^{-4}/s, 5×10^{-4}/s, 1×10^{-3}/s, 5×10^{-3}/s, 1×10^{-2}/s. On average, three specimens per strain rate are tested. The specimen design and testing procedure conform to ASTM E8 standards [12]. Dimensions of the specimen are shown in Fig. 2. The austenitic stainless steel considered for the study is equivalent to SS-321 which has a material composition listed in Table 1.

Photographs of a specimen before and after testing are shown in Figs. 3 and 4, respectively.

Fig. 1 Photograph of universal testing machine

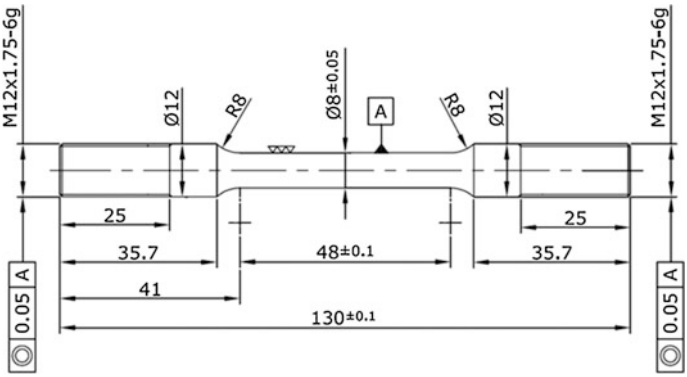

Fig. 2 Dimensions of the tension test specimen

Table 1 Material composition of SS-321

Alloying element	% by weight
Carbon	0.12 max
Chromium	17–19
Nickel	9–12
Titanium	0.7 max
Iron	Balance

Fig. 3 Specimen before testing

Fig. 4 Specimen after testing

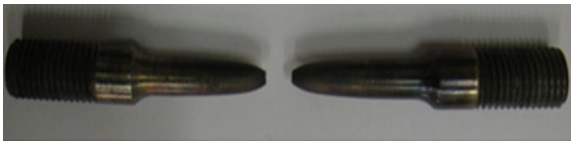

The stress–strain curve, yield and ultimate strengths, percentage elongation and percentage reduction in area of each specimen are recorded from the tests. A total of 15 specimens are tested. Stress–strain curves at each strain rates tested are shown in Fig. 5. The average yield strength at each strain rate is listed in Table 2, and the variation of yield strength with strain rate is illustrated in Fig. 6. The static yield strength (yield strength corresponding to zero strain rate) is found to be 199.2 N/mm^2 which is obtained by extrapolating the curve in Fig. 6 to zero strain rate.

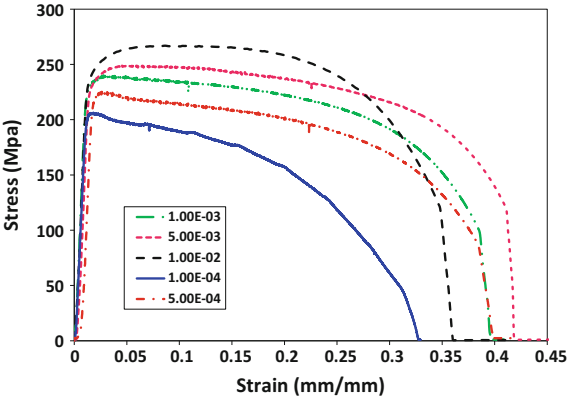

Fig. 5 Stress–strain graphs at different strain rates

Table 2 Average yield strength from tension tests

Strain rate (mm/mm/s)	Yield strength (N/mm^2)
1×10^{-4}	206.03
5×10^{-4}	218.63
1×10^{-3}	221.75
5×10^{-3}	227.43
1×10^{-2}	235.4

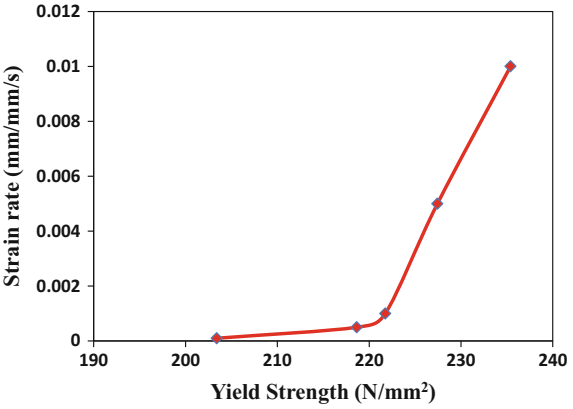

Fig. 6 Variation of average yield strength with strain rates

4 Determination of Perzyna Parameters

The Perzyna model parameters are evaluated based on the methodology reported by Klosowski and Mleczek [10]. The logarithmic values of (stress ratio-1) and strain rate are determined and are plotted in linear scale as shown in Fig. 7 so that the equation for the linear curve is obtained.

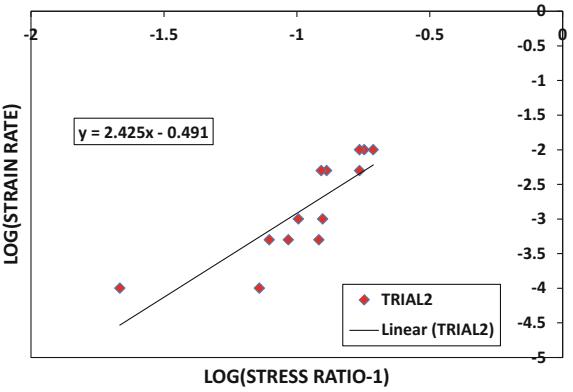

Fig. 7 Determination of Perzyna parameters

The equation for the linear curve is

$$y = 2.425x - 0.491 \tag{4}$$

By taking logarithm on both sides of Eq. 3 and rearranging, we get:

$$\log \dot{\varepsilon} = \frac{1}{m} \log \left(\frac{\sigma_d}{\sigma_s} - 1 \right) + \log D \tag{5}$$

By comparing Eqs. 4 and 5, we get:

$$1/m = 2.425, m = 0.412, \log D = -0.491, D = 0.322$$

The Perzyna model for the stainless steel can thus be expressed as:

$$\dot{\varepsilon} = 0.322 \left(\frac{\sigma_d}{\sigma_s} - 1 \right)^{1/0.412}. \tag{6}$$

5 Numerical Examples

This section covers two examples to illustrate viscoplastic modeling and analysis. The specimen geometry, material model adopted and different load cases considered are discussed below.

5.1 Stress Analysis of a Tension Specimen Under Monotonic Loading

The purpose of this exercise is to validate the above-developed viscoplastic model. It is done by comparing actual tension tests with Perzyna based finite element simulations. Due to the symmetry of the tension test specimen (see Fig. 2) along axes *X* and *Y*, a quarter portion is idealized as illustrated in Fig. 8. Four noded axisymmetric solid elements PLANE182 are used for meshing. Perzyna model is combined with the rate-independent multi-linear isotropic hardening (MISO) plasticity model for analysis of monotonically loaded structures. The material properties used are shown in Table 3, and MISO model graph is shown in Fig. 9. True stress–true strain properties corresponding to a strain rate of 1×10^{-3}/s are used for MISO modeling.

All the nodes along the line AD are arrested in the radial direction, while the nodes along line CD are supported in the axial direction (refer Fig. 8). All the nodes along line AB are coupled together and pulled up in Y direction to simulate the displacement loading pattern as in a UTM. A small reduction in diameter is modeled at mid-length of the specimen in order to force the neck formation at this location. Displacement loading is applied on the top nodes in increments till the specimen failed. Failure is indicated by a non-convergence of equilibrium iterations signaling tensile rupture of the specimen. The following investigations are made:

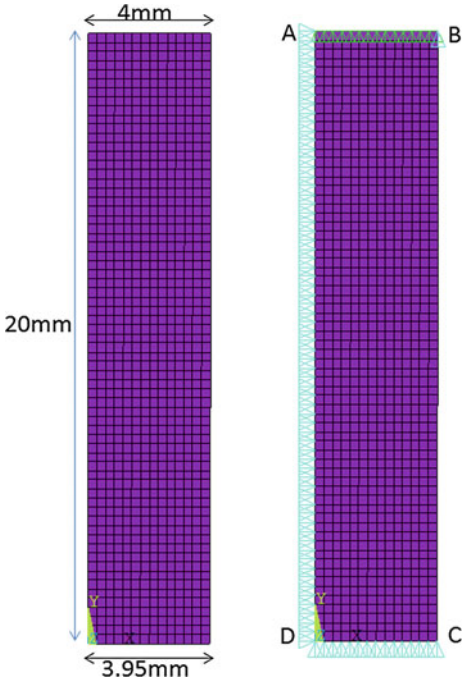

Fig. 8 FE model and boundary conditions

Table 3 Viscoplastic properties used for SS-321

Property	Value	Unit
E	105582.2	MPa
v	0.3	–
m	0.412	–
D	0.322	mm/mm/s

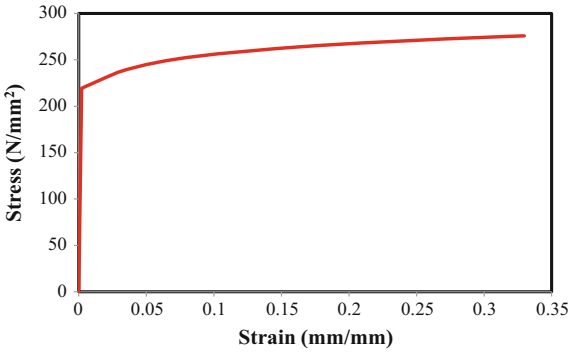

Fig. 9 MISO model graph for SS-321

- Sensitivity study of duration of application of load
- Sensitivity study of parameter m
- Sensitivity study of parameter D
- Comparison of stress–strain behavior with actual tension test results.

Sensitivity study of duration of application of load

Different durations are considered from 40 to 40000 s (strain rate ranging from 0.01 to 0.00001 mm/mm/s) for load application, and the stress–strain graphs plotted for each case. The plots are compared with the experimental stress–strain curve for the strain rate of 1×10^{-3} mm/mm/s, the actual duration of application of load being 400 s. An elastoplastic analysis is also done without considering the Perzyna model. This graph is also included in Fig. 10. From this figure, it is clear that duration of application of load has got a significant effect on the stress–strain response. It can be seen that as duration increases the yield strength decreases (i.e., as strain rate reduces, the yield strength decreases). The shape of simulation curve matches fairly with the test curve for a duration of 130 s.

Sensitivity study of parameter *m*

In order to study the effect of parameter m, simulations are run with m ranging from 0.162 to 0.612. Duration considered for this study is 400 s. The value of m could not be decreased below 0.162 due to computational difficulties. Stress–strain graphs plotted for different values of m are illustrated in Fig. 11. From this figure, it is observed that as m approaches zero, the effect of viscoplasticity becomes predominant while as the value approaches one the viscoplastic effect is lower. For a value of 0.212, the test curve matches well with the simulation curve up to a strain of 0.3 mm/mm.

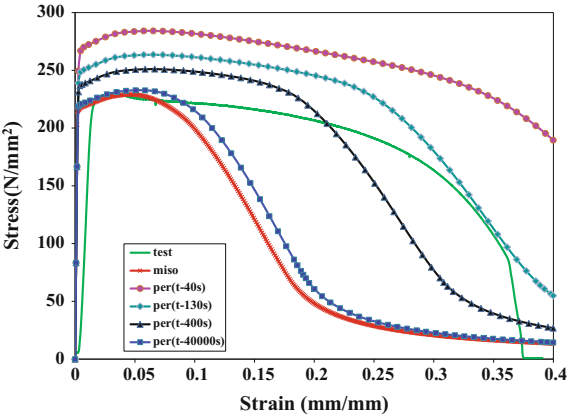

Fig. 10 Sensitivity study of load application duration

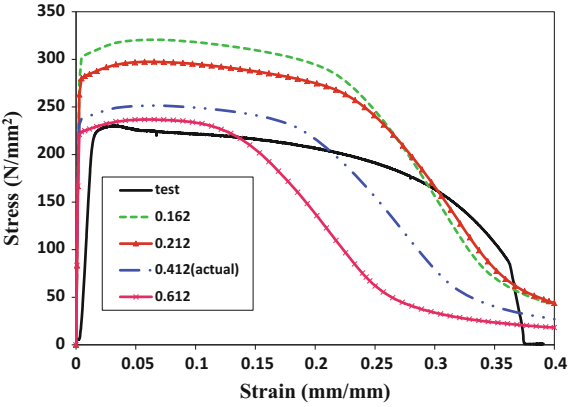

Fig. 11 Study of parameter *m*

Sensitivity study of parameter *D*

D is varied from 0.012 to 0.522/s. The obtained stress–strain curves are plotted along with the test curve as shown in Fig. 12. It is found that as *D* decreases the yield strength increases. It can be seen that the shape of the simulation curve matches fairly with the test curve for $D = 0.082$/s.

Validation of Perzyna model

Validation of the above-developed Perzyna model is done by comparing ANSYS simulations with test results. The stress–strain graph obtained with $m = 0.412$ and $D = 0.322$/s at a strain rate of 1×10^{-3} mm/mm/s for the actual test duration of 400 s is plotted in Fig. 13 together with the corresponding test graph. It is found that both the graphs do not match well. However, for a simulated test duration of 130 s, the test graph and Perzyna prediction match reasonably. This indicates that the fitted values of $m = 0.412$ and $D = 0.322$/s based on tension test data derived from 15 specimens do not represent the true viscoplastic behavior of the material. Therefore, a larger number of specimens should have been tested to get better

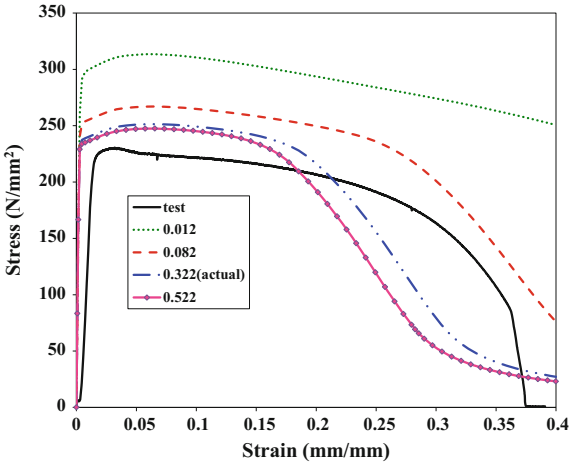

Fig. 12 Study of parameter *D*

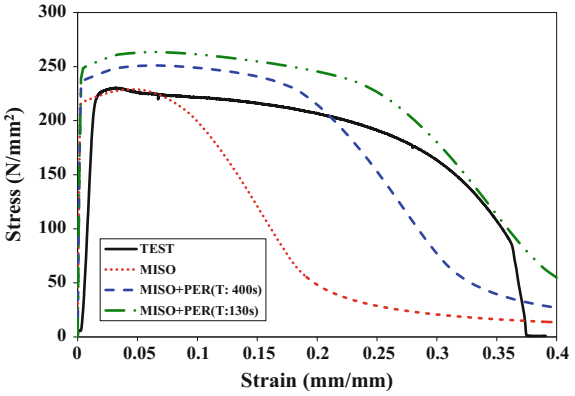

Fig. 13 Validation of Perzyna model for tension specimen

estimates of the Perzyna parameters. However, the Perzyna model gives a better stress–strain response for the stainless steel tested compared to the MISO-based classical plasticity model which gives an odd pattern of the stress–strain graph after peak stress point.

5.2 *Cyclic Stress Analysis of a Simple Block*

The following material models are studied to check their suitability for analysis of cyclically loaded structures:

- Chaboche nonlinear kinematic hardening plasticity model [8]
- Chaboche + Perzyna model

- Chaboche + Voce model [13]
- Chaboche + Voce + Perzyna model.

A single plane stress element is used for two-dimensional cyclic stress analysis with an element size of 1 mm as shown in Fig. 14. Displacement loading of ±0.05 mm is applied on one edge of the element for two cycles as shown in Fig. 15. The cyclic stress–strain graph obtained using the above material model combinations is shown in Fig. 16. From this figure, it is observed that a combination of Chaboche, Voce and Perzyna models is well suited for modeling cyclic plasticity combined with viscoplasticity. The stress corresponding to a given strain with this model is found higher compared to other models.

Sensitivity study of *m* and *D*

Sensitivity study of m and D parameters is conducted for cyclic loading of the simple block with a combination of Chaboche, Voce and Perzyna models. Different values for m and D are investigated, and the corresponding stress–strain graphs are plotted as shown in Fig. 17. It is found that as m decreases while keeping D constant, the yield strength increases. Similarly, as D decreases, keeping m constant, the yield strength increases.

Thus, the Perzyna model as implemented in ANSYS could be successfully used in association with a combination of Chaboche and Voce cyclic plasticity models to analyze cyclically loaded structures.

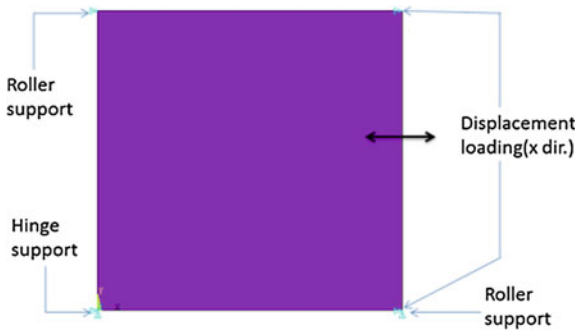

Fig. 14 FE model of 2D block

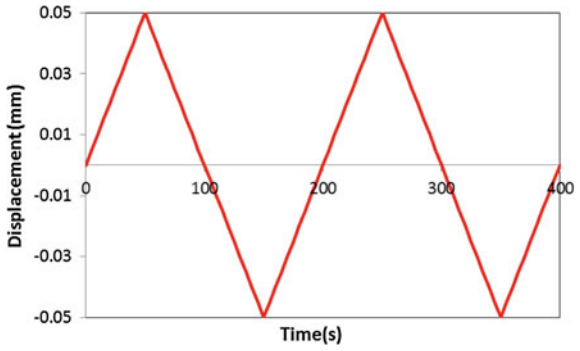

Fig. 15 Cyclic displacement loading pattern

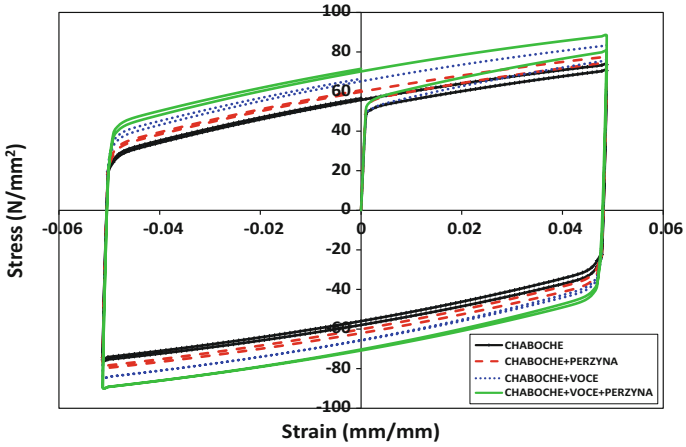

Fig. 16 Stress–strain graph for different material models

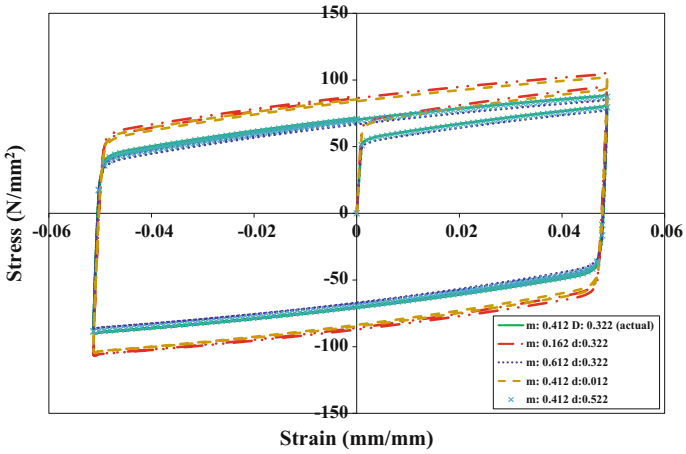

Fig. 17 Results of sensitivity study of m and D parameters

6 Calibration of Chaboche and Voce Model Parameters of SS-321

For simulating cyclic hardening of a material, it is required to combine the Chaboche nonlinear kinematic hardening model with the Voce nonlinear isotropic hardening model.

Chaboche model: To model smooth nonlinear stress–strain behavior, the Chaboche model, as given below, is commonly used:

$$\alpha_i = \frac{2}{3} C_i \varepsilon^p - \gamma_i \alpha dp \tag{7}$$

where α = back stress, dp = accumulated plastic strain, c, γ = material parameters. A third-order Chaboche model is found sufficient and hence used for the current idealization as given below:

$$\alpha = \sum_{i=0}^{3} \alpha_i \tag{8}$$

A third-order Chaboche model has 7 parameters σ_0, C_1, γ_1, C_2, γ_2, C_3 and γ_3.

Voce model: This model is used for materials exhibiting a smooth exponential transition from the linear elastic region to a final constant linear strain hardening slope. It is given below:

$$\sigma_y = k + R_o \varepsilon^p + R_\infty \left(1 - e^{-b\varepsilon^p}\right) \tag{9}$$

where σ_y = yield strength, ε^p = plastic strain, k = elastic limit (initial yield point, which is the first tensile peak stress point in the cycling), R_o = slope of linear plastic region, R_∞ = stress intercept, b = exponential hardening term. The specialty of this model is that it can represent cyclic hardening or softening of a material when combined with the Chaboche model resulting in the translation and expansion of yield surface.

In the combined Chaboche–Voce model, the former one represents the characteristics of the stabilized stress–strain graph (hysteresis loop), while the latter simulates the cyclic hardening (or softening) of the material from the virgin state to the final state. These parameters are calibrated by performing a cyclic stress analysis of a simple block under displacement loading (uniaxial tension–compression loading), and the resulting cyclic stress–strain graph is compared with the LCF test results. The parameters are adjusted by trial and error till both the curves match well.

The FE model of the simple block made of SOLID185 element is shown in Fig. 18. Figure 19 represents the cyclic displacement load used for calibration studies. The steps involved in the calibration process of SS-321 at 1000 K and strain rate of 1×10^{-3} mm/mm/s are as under:

- Step 1: LCF cyclic stress–strain graph of SS-321 at 1000 K is plotted using MS Excel. Yield strength is noted. The stress–strain curve got stabilized after a few number of cycles.
- Step 2: From the LCF test results, it is possible to plot a graph with cycle number versus peak tensile stress in each cycle as shown in Fig. 20. This graph gives the cyclic hardening or softening characteristic of a material as well its cyclic stabilization. The cycle number at which the graph becomes stabilized can be found out from this curve. It is found that at the tenth cycle, the graph got stabilized.

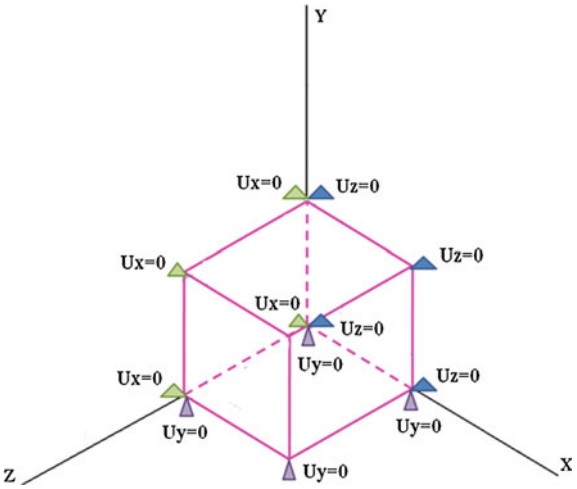

Fig. 18 FE model of a simple block

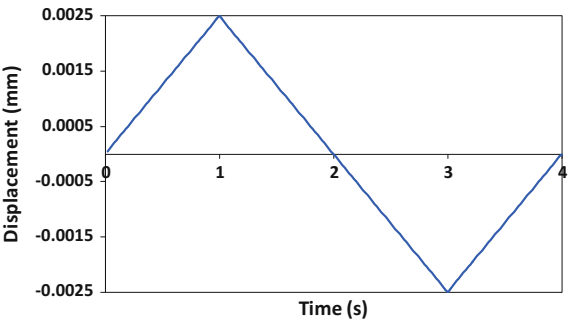

Fig. 19 Cyclic displacement load

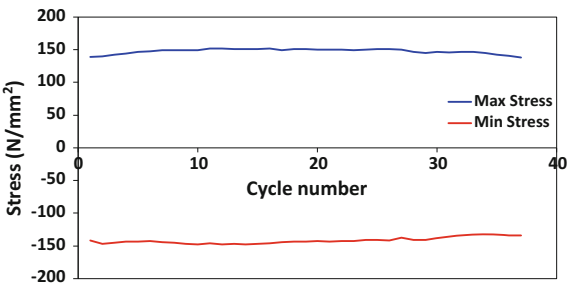

Fig. 20 Cycle number versus peak tensile stress graph

- Step 3: The stabilized cyclic stress–strain graph is plotted in this step. A sample cyclic stress–strain graph and the procedure for evaluation of the Chaboche model constants are shown in Fig. 21.

The cyclic stress–strain graph typically consists of three regions: (I) a linear elastic region, (II) a curvilinear transition from elastic to elastoplastic region and (III) a gently curved strain hardening region. Initial values of the six Chaboche model parameters are taken as follows: C_1 is taken as the slope at the beginning of region I, C_2 as the slope at the middle of region II, and C_3 as the slope of region III. γ_1 is taken as the rate at which C_1 reduces decays to C_2, γ_2 is the rate at which C_2 decays to C_3, and γ_3 is the rate at which C_3 decays. With the above-evaluated initial values of the Chaboche model parameters, a cyclic stress analysis of the simple block under uniaxial tension–compression is conducted, under displacement- or strain-controlled loading for a strain range of ±0.5% (displacement = 0.005 × 0.5 = 0.0025 mm). From this analysis, the stabilized stress–strain graph can be obtained. The Chaboche model parameters are fine-tuned by comparing the computed cyclic stress–strain curve with the LCF test results as shown in Fig. 22. This is done by trial and error till both curves match reasonably. The final values of Chaboche model parameters are tabulated in Table 4.

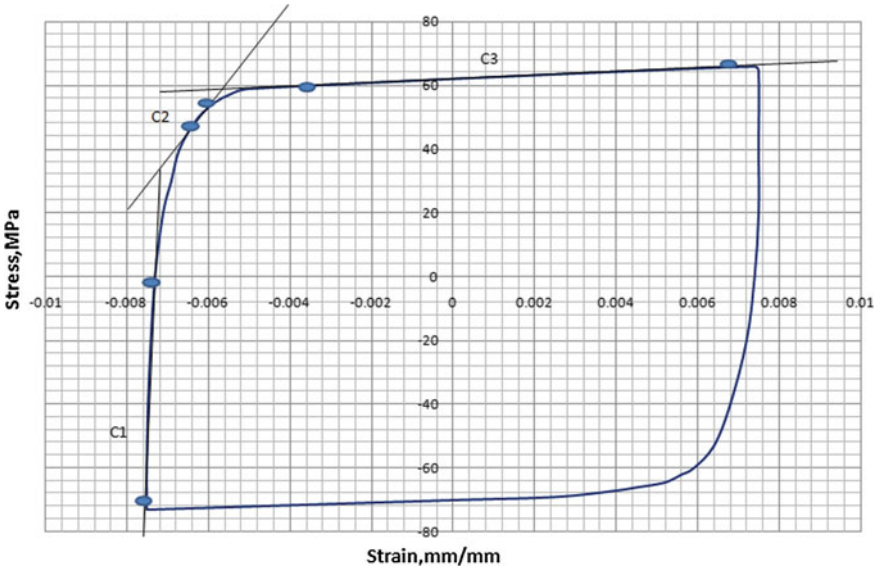

Fig. 21 Graphical method of evaluation of initial Chaboche parameters

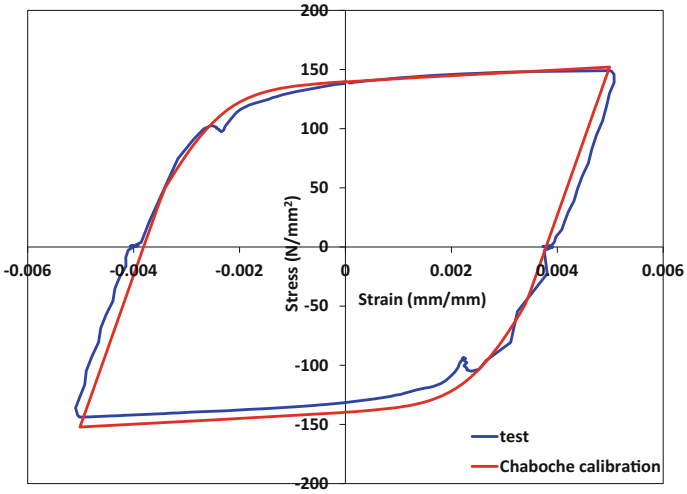

Fig. 22 Comparison of Chaboche graph with test graph

Table 4 Calibrated Chaboche and Voce parameters

Chaboche	Parameter	C_1	γ_1	C_2	γ_2	C_3	γ_3	σ_o
	Value	55000	2750	45000	1940	2500	5	130
Voce	Parameter	K	R_o	R_∞	b	–	–	–
	Value	90	0	10	20	–	–	–

- Step 4: The original Voce model relates the variation of yield stress against plastic strain as seen in Eq. 9, but in the absence of this information, we can fit an approximate equation for peak tensile stress against cycle number as described in Step 2. Since the material stabilizes to a constant stress–strain graph, the slope of the curve in the plastic region, R_0, would be zero. Only one parameter b needs to be fitted from the above curve based on trial and error.
- Step 5: Now do a combined Chaboche exact model and Voce approximated model modeling of the material and perform cyclic stress–strain analysis till stabilization of stress–strain graph is achieved. The Voce model parameters b can be calibrated by trial and error by comparing the computed cyclic stress–strain graph with the LCF test results. Analysis is continued till a reasonable match is obtained between the two curves as shown in Fig. 23. Table 4 shows the calibrated Voce parameters.

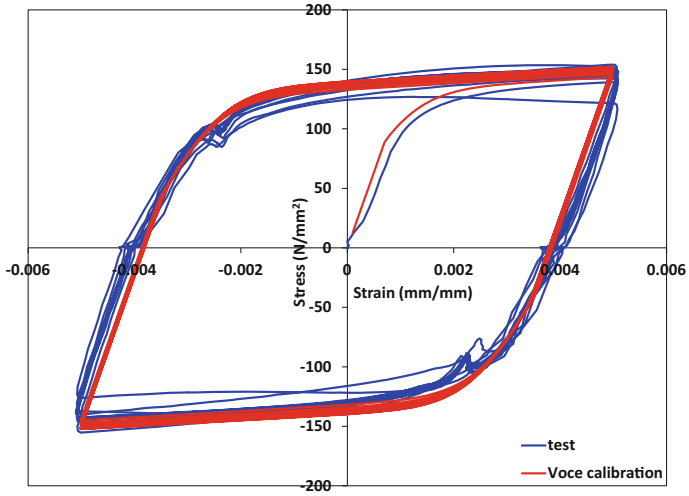

Fig. 23 Comparison of Chaboche and Voce simulations with test results

7 Cyclic Stress Analysis of Thrust Chamber

Thrust chamber is one of the important subsystems of a rocket engine. The thrust chamber generates propulsive thrust force for the flight of the rocket by ejection of combustion products at supersonic speeds. A double-walled construction is employed for these chambers where in the inner wall and ribs are made up of copper alloy up to area ratio 10 and stainless steel beyond area 10. The outer walls are made up of stainless steel throughout. The pressure and temperature load varies throughout the length of the chamber. So a section which experiences maximum temperature is taken for the cyclic stress analysis which is at area ratio 100. As the temperature is high, this location will experience viscoplastic effect.

FE model of a cyclic symmetric sector of the chamber cross section, with appropriate circumferential symmetric boundary condition, is used for analysis as shown in Fig. 24. Two-dimensional plane strain model of the thrust chamber cross section is modeled using PLANE182 elements. Two-dimensional analysis is carried out using Chaboche + Voce and Chaboche + Voce + Perzyna material model combinations, and the results are compared. Analysis is carried out considering temperature and pressure loads during seven stages of a single hot run of the engine: (a) pre-cooling, (b) ignition start, (c) hot test condition, (d) hold time for 7200 s (720 s with a factor of safety of 10), (e) initiation of shutdown, (f) post-cooling, (g) back to ambient. Duration of application of all loads except hold period is considered to be 1 s. Analysis is done for two hot tests. With these loads, the cyclic life of the thrust chamber is computed using both the model combinations. Figure 25 shows the hoop cyclic stress–strain curves at mid-channel gas side wall for two cycles of both the models combinations.

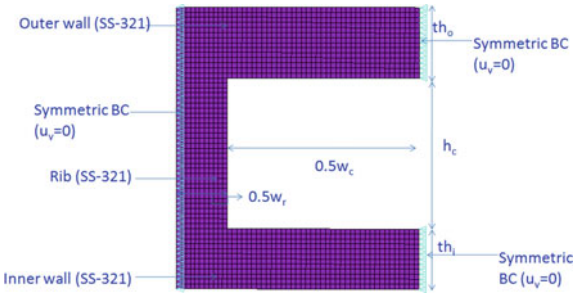

Fig. 24 Plane strain model of thrust chamber cross section

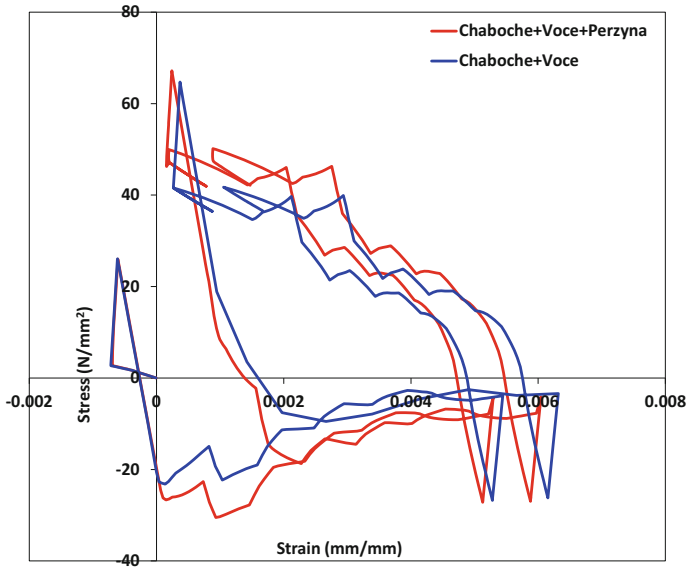

Fig. 25 Hoop cyclic stress–strain graph

From Fig. 25 it is observed that the hoop stress corresponding to Perzyna model is higher and strains lower compared to the model without Perzyna model. Also peak strain at the end of the third load step is lower by 1.5E−04.

7.1 Life Cycle Prediction of Thrust Chamber

The failure mechanisms, viz. LCF and ratcheting, contribute by varying degrees to the failure of the chamber. These damages are summed up to get the total damage

(known as cumulative damage technique), the reciprocal of which gives the life of the chamber.

- Low-cycle fatigue damage: Damage due to LCF is simply the reciprocal of the number of cycles to fatigue failure as expressed below:

$$D_{\mathrm{LCF}} = \frac{1}{N_f} \tag{10}$$

$$\text{where } N_f = \left(\frac{\varepsilon_f}{2\Delta\varepsilon}\right)^2 \tag{11}$$

ε_f is the fracture strain expressed as

$$\varepsilon_f = \ln\left(\frac{1}{1-\mathrm{RA}}\right) \tag{12}$$

where RA is the reduction in area in fraction form and $\Delta\varepsilon$ is the strain range expressed as $\Delta\varepsilon = \varepsilon_{\max} - \varepsilon_{\min}$.

For a temperature of 1000 K and strain rate of 1×10^{-3}mm/mm/s RA = 0.867, ε_f = 2.019 and $\Delta\varepsilon$ is obtained from Fig. 26. Considering a factor of safety of 4, $D_{\mathrm{LCF}} = 1.43 \times 10^{-4}$ (for Chaboche + Voce combination) and 1.36×10^{-4} (for Chaboche + Voce + Perzyna combination).

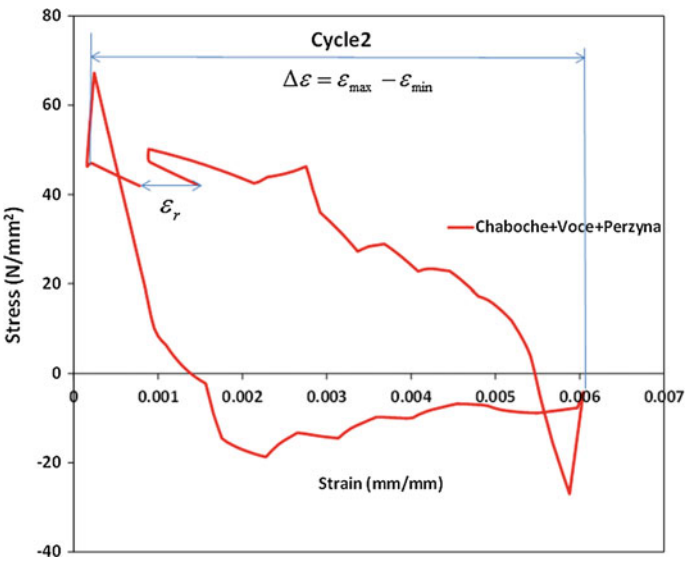

Fig. 26 Determination of strain range

- Ratcheting damage: It is the ratio of accumulated plastic tensile strain in a cycle to the fracture strain of the material. It is expressed as:

$$D_{\text{ratchetting}} = \frac{\varepsilon_r}{\overline{\varepsilon_f}} \tag{13}$$

where ε_r is the ratcheting strain (as shown in Fig. 26) and $\overline{\varepsilon_f}$ is the elongation (37.53% for 1×10^{-3}mm/mm/s).

Thus, $D_{\text{ratcheting}} = 2.09 \times 10^{-3}$ (for Chaboche + Voce combination) and 1.87×10^{-3} (for Chaboche + Voce + Perzyna combination).

- Total damage is obtained as $D_{\text{tot}} = 4 \times D_{\text{LCF}} + 2 \times D_{\text{ratcheting}}$ where 4 and 2 are the factor of safety considered for LCF and ratcheting, respectively. Number of cycles to failure is the reciprocal of total damage expressed as

$$N_f = \frac{1}{D_{\text{tot}}} \tag{14}$$

N_f is obtained as 210 (for Chaboche + Voce combination) and 233 (for Chaboche + Voce + Perzyna combination).

Study on duration of load application: The material model considered for this study is a combination of Chaboche, Voce and Perzyna models. Duration of application of load steps is varied from 1 to 3 s. It is found that the corresponding life decreases from 233 to 225 cycles.

8 Conclusion

Perzyna viscoplastic model parameters are calibrated for an austenitic stainless steel using the methodology reported by Klosowski and Mleczek from tension tests conducted at 1000 K, at different strain rates. These parameters are validated by comparing actual tension tests with finite element simulations using ANSYS. Increase in dynamic yield strength of the material due to strain rate effects is clearly seen both in tests as well as in numerical simulations. A combination of Perzyna and MISO model is found to give good results for simulating monotonic loading. For cyclic loading, Perzyna model combined with Chaboche nonlinear kinematic hardening model and Voce nonlinear isotropic hardening model is found excellent. The sensitivity of parameters 'm' and 'D' in the Perzyna model is also investigated. It is found that when 'm' and 'D' reduce, the rate-dependent effects increase. Calibration of Chaboche and Voce parameters at 1000 K for a strain rate of 1×10^{-3} mm/mm/s and strain range of $\pm 0.5\%$ has also been done.

Cyclic stress analysis of a double-walled rocket engine thrust chamber has been performed for a region which experiences high temperature. The material model used for the viscoplastic analysis is a combination of Perzyna, Chaboche and Voce models, whereas only the Chaboche–Voce model combination is used for classical elastoplastic based thermostructural analysis. Plane strain model of the required cross section is adopted for both the analyses. Number of cycle to low-cycle fatigue failure is found to be 210 for Chaboche + Voce combination and 233 for Chaboche + Voce + Perzyna combination. When the duration of application of load steps is varied from 1 to 3 s, the corresponding cycle life varies from 233 to 225 cycles. It is also observed that the hoop stress corresponding to Perzyna model is higher and strains lower compared to the model without Perzyna model. Because of this, the predicted cyclic life is higher for Perzyna model.

Acknowledgements The second author gratefully thanks Director, LPSC/ISRO, for granting permission to do her M. Tech thesis. Thanks are also due to Dr. R. Muthukumar, Deputy Director, MDA/LPSC, for permitting her to use the creep test facility and computational resources of SDAG for this work.

References

1. Wu HC (2005) Continuum mechanics and plasticity, vol 3, 2nd edn. CRC Press Company, Washington D.C., pp 225–231
2. Safari AR, Forouzan MR, Shamanian M (2013) Thermo-viscoplastic constitutive equation of austenitic stainless steel 310s. Comput Mater Sci 68:402–407
3. Lubliner Jacob (2008) Plasticity theory. Dover Publications Inc., New York, pp 117–150
4. Nordberg H (2004) Note on the sensitivity of stainless steels to strain rate. Avesta Polarit Research Foundation, Research report no. 04.0-1
5. ANSYS Mechanical APDL (2015) Version 15. ANSYS Inc, USA
6. Perzyna P (1968) Fundamental problems in viscoplasticity. Adv Appl Mech Acad Press 9:313–377
7. Lin RC, Betten J, Brocks W (2006) Modeling of finite strain viscoplasticity based on the logarithmic corotational description. Arch Appl Mech 75:693–708
8. Chaboche JL (1989) Constitutive equations for cyclic plasticity and cyclic viscoplasticity. Int J Plast 5(3):247–302
9. Yang L, Luo Y (2008) Constitutive model depending upon temperature and strain rate of carbon constructional quality steels. J Central South Univ Technol 15:43–46
10. Kłosowski P, Mleczek A (2014) Parameters Identification of Perzyna and Chaboche viscoplastic models for aluminum alloy at temperature of 120 °C. Eng Trans 62(3):291–305
11. Yang J, Chen T, Jin P, Cai G (2014) Influence of the startup and shutdown phases on the viscoplastic structural analysis of the thrust chamber wall. Aerosp Sci Technol 34:84–91
12. Anonymous (2015) ASTM-E8/E8M-15a, Standard test methods for tension testing of metallic materials. American Society for Testing and Materials, Philadelphia, USA
13. Voce E (1955) A practical strain-hardening function. Metallurgia, pp 219–225
14. Asraff AK, Sheela S, Paul A, Mathew A, Savithri S. Cyclic stress analysis of a rocket engine thrust chamber using Chaboche, Voce and Creep constitutive models. Trans Indian Inst Metals 69(2)2:495–500

http://www.springer.com/978-981-10-6001-4

Proceedings of Fatigue, Durability and Fracture Mechanics

Seetharamu, S.; Rao, K.B.S.; Khare, R.W. (Eds.)

2018, XII, 471 p. 320 illus., 222 illus. in color.,
Hardcover
ISBN: 978-981-10-6001-4